Adhesion at the Solid–Elastomer Interface: Influence of the Interfacial Chains

M. Deruelle,[†,‡] L. Léger,[*,†] and M. Tirrell[*,‡]

Laboratoire de Physique de la Matière Condensée, Collège de France, URA CNRS 792, 11 Place Marcelin Berthelot, 75231 Paris Cedex 05, France, and Department of Chemical Engineering and Materials Science, University of Minnesota, Minneapolis, Minnesota 55455

Received December 28, 1994; Revised Manuscript Received July 12, 1995[⊗]

ABSTRACT: We have studied the adhesion between an elastomeric lens of cross-linked poly(dimethylsiloxane) (PDMS) brought into contact with a silicon wafer covered by a grafted layer of monodisperse PDMS. The influence on the adhesion of the molecular weight and the surface density of the grafted chains was examined by modifying them independently. The mechanical test we used was the JKR method, which measures the variation of the radius of the contact area, a, between the wafer and the lens as a function of P, the load applied. This technique gives the dependence of the interfacial adhesion energy, or strain energy release rate, G, on the crack propagation speed, V. We modified the apparatus commonly used to operate at constant, imposed displacement in an effort to obtain data at the lowest possible loads and deformations. Recording of a and P as a function of time enabled the determination of G as a function of V down to speeds as low as 5 nm/s. Our results show that G still depends on V, even in the lowest range of speeds. If we refer to the low-velocity values of strain energy release rate as adhesion energies, G_0, we find that G_0 is affected strongly by the grafted layer and apparently governed by the ability of the chains from the grafted layer to penetrate the network. The adhesion energies we measure are invariably higher than that expected from accounting for only the surface energy of PDMS. Layers grafted from the melt state over a range of molecular weights, where the grafted chains have their unperturbed dimensions, show less adhesion enhancement than do layers of the same thickness produced by grafting high molecular weight polymers from a range of solution concentrations, which results in compressed configurations of the grafted chains when the solution grafted layers are dried. There appears to be a thickness for the grafted layers which is optimum in generating adhesion enhancement between the lens and the wafer. By modifying the nature of the network, we have shown that the structure of the elastomer plays an important role in determining the adhesion energy.

Introduction

Interfacially anchored chains are effective in promoting the adhesion between rubbers and other solids.[1,2] Other interfacial mechanical properties, such as sliding friction, between elastomers and solids may also be manipulated by interfacial chains.[3–6] Means of attaching chains to interfaces and our understanding of the structures of such interfacial layers have increased substantially recently.[7] Our aim is to use this structural knowledge to enhance mechanistic understanding of interfacial properties.

The current situation regarding solid–elastomer adhesion has been well summarized recently by Brown.[8,9] At interfaces involving elastomeric polymers, the measured adhesion energy is always a strong function of the rate of crack propagation. The measured adhesion can be very high and strongly dependent on rate of crack growth, even if only van der Waals forces join the interface. Interfacial chains, or connectors, that cross the interface (for example, polymer chains grafted by their ends to an otherwise impenetrable solid) and couple physically by interpenetration and possible entanglement (for example, with a elastomer) raise the measured adhesion energy further. The questions of current interest begin when one tries to advance from this generally accepted observation. We confine ourselves here to conditions well above the glass transition temperature of the elastomeric component and where the mechanism of interfacial failure does not involve any chain scission, that is, failure occurs by chain pullout (for insight into cases where these conditions are not met, see refs 10 and 11).

Determination of the dependence of the interfacial fracture energy on the number density and length of connecting chains and on the rate of crack propagation is an important objective, in a practical sense, since these are controllable variables, and in a fundamental sense, since there are theoretical models available predicting these dependences, but which have as yet had little confrontation with experimental data. The models,[12,13] as discussed by Brown,[9] all assume that a threshold stress exists below which chain pullout does not occur. There is, in this view, a threshold toughness, or adhesion energy, G_0, which obtains at low speed, V, of crack growth. Above a critical speed, V^*, the interfacial adhesion energy, G, increases above G_0. The models differ in what they assume about the state of the chains after pullout and in the details of the analysis of the elastic fracture problem. The rate of growth of G above V^* is predicted to depend[4,13] on the nature of the intermingling among the interfacial chains. Brown's recent work[9,14] provides data relevant to these models; he examined the adhesion of cross-linked polyisoprene to surfaces prepared with varying densities and fixed length of tethered linear polyisoprene to surfaces prepared with varying densities and fixed length of tethered linear polyisoprene connector chains. He did not see clear evidence for a V^* (though the estimated it to be at the low end of his experimental range, in the neighborhood of 0.3 nm/s; see also ref 15 for a similar observation), so he determined a G_0 experimentally by extrapolation of his G versus V data (which appeared to be reasonably linear) to zero velocity. The interfacial

[†] Laboratoire de Physique de la Matière Condensée, Collège de France

[‡] Department of Chemical Engineering and Materials Science, University of Minnesota

[⊗] Abstract published in *Advance ACS Abstracts,* September 15, 1995.

0024-9297/95/2228-7419$09.00/0 © 1995 American Chemical Society

adhesion energy, both at zero velocity (G_0) and at finite velocity, grew with the areal density (Σ) of connector chains, appearing to saturate for this particular connector length around 0.05−0.1 nm^{-2} at a value of G approaching 10 times the $\Sigma = 0$ value. G_0 increased less rapidly with Σ, augmenting by a factor of about 3, over the same range of Σ. Consistent with this, he obesrved, too, that the slope, dG/dV, increased faster than linearly with areal density of connectors. Brown concluded that the linear dependence of G on V was in agreement with several of the models, whereas the value of dG/dV was consistent only with the ideas that the connectors cross the interface several times.[13] In more recent work,[14] analyzing additional data, Brown et al. argued that the high effective friction they observed at low V may be more related to the dynamics of chain pullout, as suggested by Rubinstein et al.,[4] than to the multiple stitching.

Many significant questions remain for exploration. The experimental dependencies of G and G_0 on Σ are yet to be established definitively. The models of de Gennes and co-workers[12,13] predict

$$G_0 - W \approx kTN\Sigma \quad (1)$$

where W is the Dupré energy, or the thermodynamically reversible work of adhesion between two surfaces A and B, equal to $\gamma_A + \gamma_B - \gamma_{AB}$, and N is the degree of polymerization of the connector chains. Brown writes[9] that his data, while not definitive on this issue, are not inconsistent with the linear dependence of eq 1; however, experimental uncertainty aside for the moment, as mentioned above, the data could also be interpreted as reaching a plateau in G_0 with increasing Σ. A major set of questions concerns the nature of the chain segments that form the connectors: how much penetration is there of the connectors into the elastomer? In other words, what short of stretch of interfacial chain actually forms the connector? How does the interfacial toughness depend on the molecular weight of the interfacial chains? Are there effects of how the interfacial chains are tethered to the solid, i.e., from a solution state or a melt state, which will affect *inter alia* the configurations of the interfacial chains? The term "connector" above is used to refer to the chains actually responsible for the adhesion enhancement; every chain grafted to the surface of the wafer and counted in the overall grafting density, Σ, may not form an effective connector. Another major set of questions concerns the interrelated issues of time and rate dependencies of the adhesive interfaces. How long does it take for grafted layer to establish a maximally effective junction with the elastomeric material? How are the dynamics of separating the junction affected by the length and density of the grafted chains and by the cross-link density of the elastomer?

The work presented here differs from that published by Brown and co-workers in several ways. Besides our choice of different materials (poly(dimethylsiloxane) (PDMS) networks and grafted chains), we perform the JKR experiment in a slightly different manner, imposing a fixed displacement on the contacting materials rather than Brown's method of unloading the sample after a specified time at fixed load. More significantly from the point of view of polymer physics, we examine two alternative ways of grafting layers on the surface of the silicon wafers, from the melt and from the solution state, both of which produce the same range of final thicknesses of the dried grafted layers, but in which the configurations of the grafted chains are different, in ways discussed further in subsequent sections. We also have varied the molecular weight between cross-links in the silicone elastomer, in a precise manner, using end-functionalized chains to make the network, to investigate directly its effect on adhesion.

Experimental Techniques

1. Preparation of the Layers. The PDMS chains used to modify the surface of the silicon wafer were α,ω-hydroxyl-terminated, with a polydispersity of approximately 1.1. They were grafted onto the native oxide of a silicon wafer by heating the layers in contact with the wafer at 120 °C for several hours and then rinsing off all unreacted material. In order to control the surface grafting density, a polymer solution of molecular weight M (or degree of polymerization N) and concentration Φ is reacted with the silica surface. It has been shown that, after rinsing, the Σ of the resulting layer scales like $N^{-1/2}\Phi^{7/8}$.[16] Two different series of substrates were studied: one was obtained by maintaining M fixed (M = 293 000 or 412 000) and varying Φ (from 5 to 100%) in the solution from which the PDMS was grafted; the other one was obtained by keeping Φ = 100% (reaction from the melt) and varying the molecular weight of the polymers grafted (from 17 000 to 500 000). The thicknesses of all dried, grafted layers were determined by ellipsometry or X-ray reflectivity.[17] It is difficult to make a precise measurement of the number of chains that are anchored at both ends. The fact that these layers swell less in good solvents than true brushes at the same areal density of chains[17] is circumstantial, not definitive, evidence for considerable attachment by two ends.

2. Preparation of the Elastomeric Lenses. The PDMS chains used were α,ω-vinyl-terminated with average molecular weights of 9600, 15 000, and 30 000 (referred to respectively as D130, D200, and D400, polydispersity of approximately 2), kindly donated to us by Carl Kessel of 3M. The cross-linker, designated D4D′5, is an oligomer consisting of four dimethylsiloxane monomers and five hydromethylsiloxane monomers. Cross-linking is effected via hydrosilation catalyzed by a platinum complex (100 ppm). In order to prevent reaction at room temperature, an inhibitor of that catalyst was also added to the mixture before heating. By varying the ratio, R, of hydride to vinyl, we obtained various elastomers with different properties. A ratio of 1.3 for D130 produced the maximum modulus and therefore was used in all of our experiments unless explicitly stated otherwise.

Lenses for the JKR adhesion experiments (described in the next section) were prepared by placing droplets of the uncured mixture onto a microscope slide that had previously been treated with chlorosilane so that the PDMS does not wet the glass, thereby producing a small spherical cap.[18] The reaction was carried out for 1 h at 70 °C. The lenses were then washed in heptane overnight. The extractable fraction generally varied from 4 to 15% depending on R; the extractable fraction was lowest for R = 1.3, which we used for all of the data reported here. The cross-linked lenses were dried in a vacuum over for 30 min. The radii of curvature of these lenses were measured by determining the height and the base of the spherical cap. The lenses employed all had radius of curvature smaller than 1 mm. The elastic constant K was determined as part of the protocol in executing the adhesion measurement described in the next section.

3. Adhesion Measurement. The JKR method of adhesion measurement[19] has received renewed attention recently[20] as a technique that is particularly well suited to investigating the surface materials and surface physical chemistry aspects, as distinct from the bulk rheological aspects, of adhesion. Chaudhury and Whitesides[18] used it to examine the effects of different surface treatments of PDMS on adhesion. Brown and co-workers[8,9,14] employed it to pioneer the examination of the effects of tethered chains on adhesion. Its desirable features in this kind of study include measurement at very low rates of deformation (in principle, measurement at zero rate is possible) and small contact areas for measurement, meaning that smooth, well-defined contact can be achieved and also that

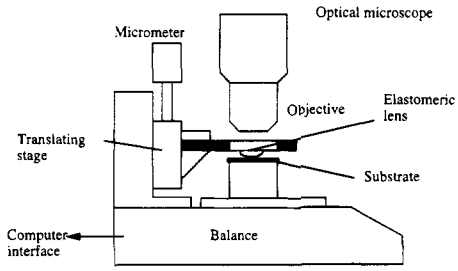

Figure 1. Schematic diagram of the experimental apparatus.

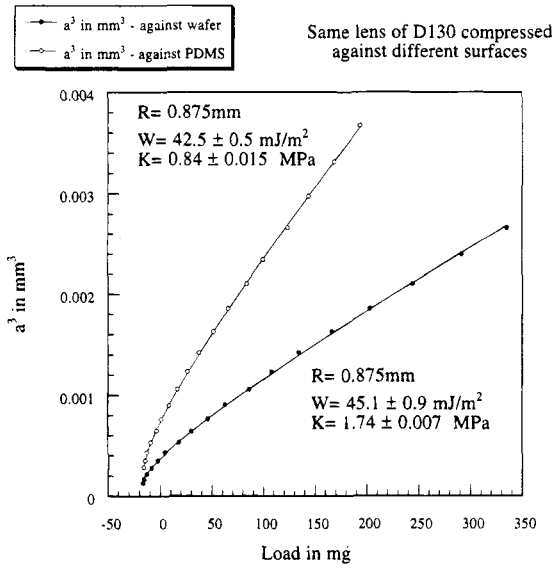

Figure 2. Contact radius versus applied load data for an identical PDMS lens against a rigid wafer surface (filled symbols) and against a flexible PDMS surface (open symbols).

a small volume of sample experiences any deformation, so that bulk dissipation effects, which are extensive in the volume of material involved, are negligible.

(a) Apparatus. The experimental apparatus is illustrated schematically in Figure 1. The lens was placed on a rigid transparent support that was fixed on a translating stage of an optical microscope (Nikon, Diaphot). The stage could be displaced vertically using a micrometer. The lenses were compressed against the substrate that was put on the plate of an analytical balance (Science Tech, Model 210). The microscope/balance combination enabled the simultaneous measurement of the contact radius and the corresponding load. The microscope operated in the reflective mode, requiring only one transparent material, either the substrate or the lens, in the contacting pair. The balance consists of an electromagnetic system maintaining the pan in a fixed position during load determination. With such a system, the quantity that is imposed on the contacting materials is in the displacement, δ (the distance by which the lens is squeezed or stretched from the position of an undeformed tangential contact between the spherical and flat surfaces), which differs from the more conventional setup where the load is imposed. The balance is interfaced with a computer to record automatically the load variations.

(b) Typical Loading Curves: Determination of K and W from the JKR Theory. Figure 2 shows typical results obtained for compression experiments where the load increases monotonically. The experimental protocol is to compress the lens against the surface, increasing δ step-by-step. After each step of compression, the system was allowed to stabilize before recording the contact radius and the load. In the data illustrated, we compressed the same lens against two different surfaces, a flat sheet of cross-linked PDMS and a rigid silicon wafer covered with a thin grafted layer of PDMS. The JKR theory[19] modifies the classical Hertz[21] result for the deformation of a sphere in contact with a flat surface (or, in general, two spheres) to include the effect of interfacial energy or work of adhesion; the result is cast in the form of the variation of the cube of the contact radius, a, with applied load, P:

$$a^3 = (R_s/K)\{P + 3\pi WR_s + [6\pi WR_sP + (3\pi WR_s)^2]^{1/2}\} \quad (2)$$

where $K = {}^4/_3\{(1 - \nu_1^2)/E_1 + (1 - \nu_2^2)/E_2\}^{-1}$, with the E_i being the Young's modulus and the ν_i the Poisson ratio of each of the two contacting materials. R_s is the radius of the undeformed sphere ($=R_1R_2/(R_1 + R_2)$ if there are two spheres of different radii). The first term of eq 2 is the Hertz result for nonadhesive surfaces; the remaining terms give the effect of adhesion energy on the contact. By determining the variation of the contact radius with applied load, it is possible to fit such data to eq 2 and to extract two independent properties, namely, the elastic constant, K, and the work of adhesion, W. The solid lines in Figure 2 trace such fits to the data, with the fitting parameters given in the figure. The fit indicates that we can determine W and K with a precision of better than 5% in this manner. The values of W thus obtained give numbers for the surface energy of PDMS (since the two contacting surfaces are chemically identical in this case, and there is no interdigitation or chemical reaction on contact, $W = 2\gamma$) that are in excellent agreement with the literature value of 21.7 mJ/m^2.[18]

Several other points are worth noticing. The first point of contact, corresponding to $\delta = 0$, gives a negative load. The surfaces attract each other such that if no constraint were applied, the bodies would come closer and increase the contact area at zero load. Here, by maintaining the two surfaces at a constant, imposed relative distance, we prevent this additional displacement due to the attraction, which results in a net tension. Note that the corresponding load at this point (assuming W is constant during unloading) is given from the JKR theory by $P_{\text{zero displacement}} = -{}^4/_3\pi WR_s = {}^8/_5P_{\text{separation}}$ (at controlled displacement) or ${}^8/_9P_{\text{separation}}$ (at controlled load), such that the loads at zero displacement or at separation can be used as independent determinations of W, in addition to eq 2. A second noteworthy point is that, in the JKR theory, the elastic constant of the system can be written $K^{-1} = K_{\text{lens}}{}^{-1} + K_{\text{subs}}{}^{-1}$, so when the substrate is a flat sheet of the same PDMS as that of the lens (curve a), $K = K_{\text{lens}}/2$, and when the substrate is a rigid wafer (the grafted layer is about 100 Å thick and thus its compliance in neglected) (curve b), $K = K_{\text{lens}}$. This factor of 2 difference between the two situations is observed in Figure 2 within the experimental error. In all of the data reported in this paper, the value of K determined from loading data was used to analyze and interpret the unloading data.

(c) Unloading Curves. Unloading experiments enable the determination of the forces to separate the two surfaces to evaluate and employ the formulas for $P_{\text{separation}}$ above. Figure 3 shows the data on unloading corresponding to curve a in Figure 2. Two kinds of unloading data are shown. In one set of data, the lens surface was supported on a very stiff, thick glass support, the necessary circumstance for enforcing the constant displacement condition; in the other data set, a thinner, flexible piece of glass was used to support the lens, in effect, transmitting to the contacting surfaces, not a controlled displacement, but a controlled load, depending on the rigidity of the glass support. Notice that the separation forces for the two conditions are, within experimetnal error, different by a factor in good agreement with the JKR-predicted value of ${}^5/_9$ from the formulas in the preceding paragraph. In all the data reported subsequently in this paper, we employed a support for the lens which could be considered infinitely stiff, yielding data at controlled displacement. Notice also that for this case, where the two surfaces are both cross-linked networks with the optimum stoichiometry of $R = 1.3$, we see negligible difference between the loading and unloading curves.

In general, unloading data on a vs P do not superimpose with loading data. Hysteresis is often observed and, in particular, is a generic feature of the data we report here on contacts between cross-linked lenses and grafted polymer

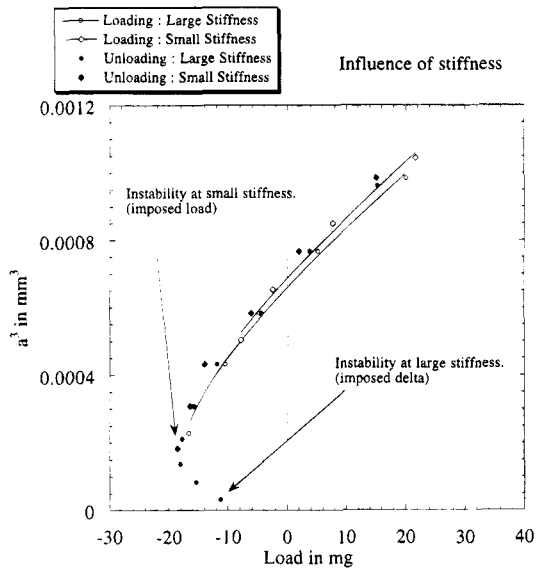

Figure 3. Contact radius versus applied load data under fixed load (diamonds) and fixed displacement (circles) in both loading (open symbols) and unloading (filled symbols) modes. The points where the contact becomes unstable on reducing the load in each mode are indicated by arrows on the figure.

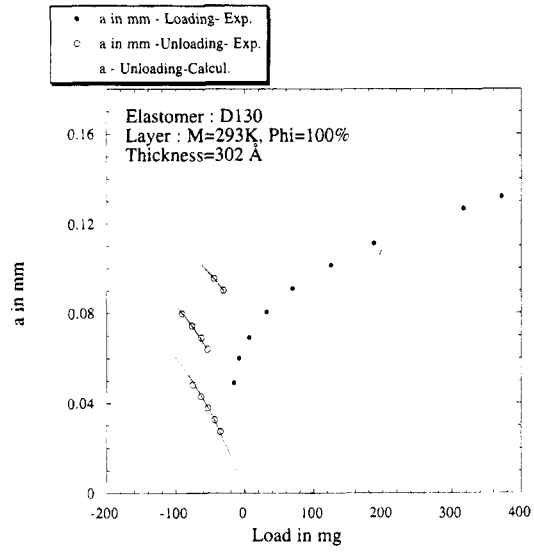

Figure 4. Typical loading and unloading data for a PDMS lens against a grafted layer of PDMS. The data are typical of all lenses and layers we have studied but these actual data are for a melt-formed PDMS layer of 293 000 molecular weight against a PDMS elastomer lens. Lightly dotted lines represent calculated trajectories for data at different fixed values of displacement, δ.

layers, for reasons discussed in more detail subsequently but, briefly, due to the increase in adhesive energy owing to intermingling between the grafted chains and the network. As illustrated in Figure 2, *these factors do not affect the loading curves*. It is therefore necessary to develop a protocol to characterize the unloading curves with respect to their rate and time dependence and to determine values of the adhesion energy during unloading.

The difference between loading and unloading data is illustrated in Figure 4 for contact between a lens and a particular grafted layer. These data are qualitatively representative of all the data in this paper. The unloading data were obtained according to the following protocol. The sample was loaded up to the maximum load, recording the loading data in the process. The surfaces were left in contact at the maximum load for 1 h (dependence of the data on time at maximum load is discussed subsequently). Unloading was realized by imposing step decrements in displacement (three

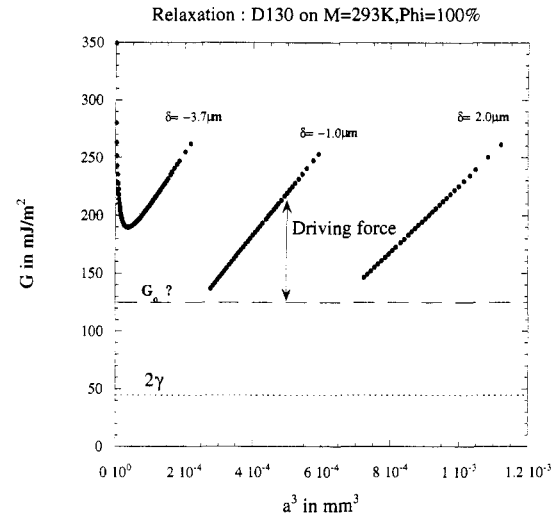

Figure 5. Strain energy release rate for different fixed values of displacement, δ. Same data as in Figure 4.

in the case of the data shown in Figure 4). Each step, which is imposed effectively instantaneously, is followed by a relaxation of the system during which the contact radius decreases and the load increases. Data on a and P are monitored during this relaxation. It is verified that the relaxation occurs at constant displacement by plugging the a vs P data into the JKR equation for displacement:[20,22]

$$\delta = a^2/3R_s + 2P/3aK \tag{3}$$

with R_s measured independently and K determined from the loading experiment. The calculated paths of constant δ relaxation are shown as the finely dotted lines in Figure 4 and they clearly superimpose on the data. Relaxation was allowed to occur as long as practicable, terminating when the further decrease in a was imperceptible on a time scale of hours or when a spurious vibration disrupted the experiment.

To analyze the unloading data quantitatively, we employ a rearrangement of the JKR eq 2 to solve explicitly for W:

$$W = (P - P_h)^2/6\pi Ka^3 \tag{4}$$

where $P_h = a^3K/R_s$ and is the so-called Hertzian load, that is, the load that would have been necessary in a purely Hertzian situation, with no adhesion between the surfaces, to produce the observed contact radius. For equilibrium data, the work of adhesion, W, is exactly matched by the strain energy release rate, G. This is the classical Griffith criterion of fracture mechanics, $G = W$. During relaxation, equilibrium does not obtain and therefore the data on a versus P correspond to a nonequilibrium value of G which is driving the relaxation of the contact of the opening of the crack as contact radius decreases. We therefore use a nonequilibrium form of eq 4

$$G = (P - P_h)^2/6\pi Ka^3 \tag{5}$$

to determine the strain energy release rate. All pairs of points in the a vs P data set can be used to calculate a value of G from eq 5 corresponding to the current values of a and P. This procedure derives from the analysis of Maugis and Barquins[20,22] and has been employed by others.[8,9,14,23] In practice, we used a small modification of this procedure. By measuring a few pairs of (a,P) points, we could determine accurately the value of δ from eq 3, as indicated in Figure 4. Knowing this value of δ, it is then only necessary to determine P as a function of time, again employing eq 3 to ascertain the corresponding value of a. Since P is recorded automatically, this procedure enabled the collection of a large data set for a given pair of surfaces relatively easily.

Figure 5 shows the values of G determined in this manner corresponding to each instantaneous value of load for the same data set illustrated in Figure 4, comprising three different

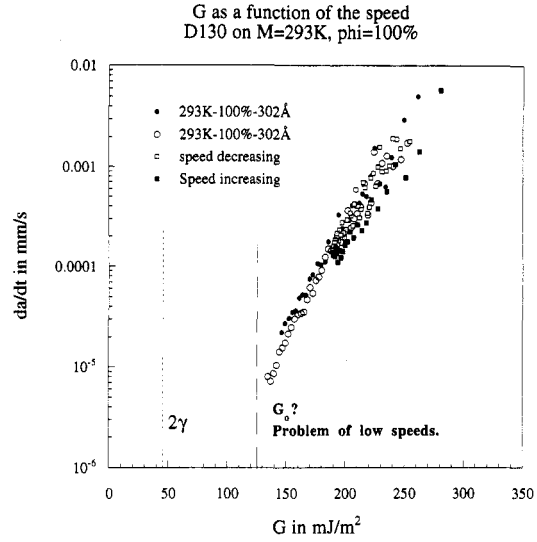

Figure 6. Data for the same system as in Figures 4 and 5 converted into the form of velocity of crack propagation (da/dt) as a function of strain energy release rate (G).

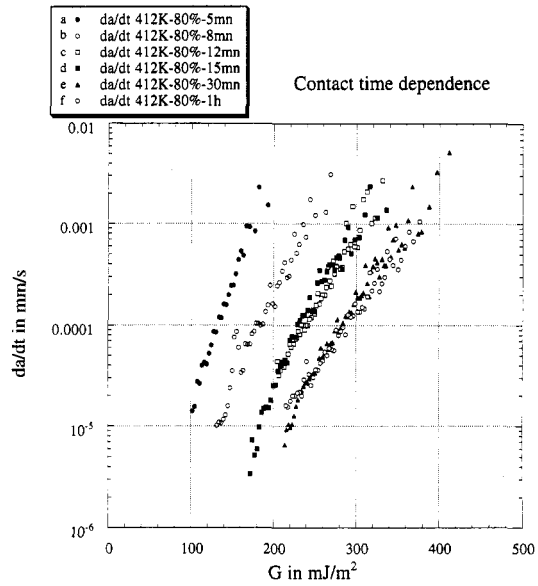

Figure 7. Data relating strain energy release rate to velocity of crack propagation for the $\Phi = 0.80$ solution-formed layer as a function of contact time between the layer and the PDMS lens.

constant values of displacement. For the two larger values of δ (curves a and b), G decreases as the contact radius shrinks. There is no obvious asymptotic limit of these data; however, one might hypothesize that the data are tending to such a value, which may be the threshold adhesive energy for the interface, at which the two surfaces would achieve an equilibrium contact. As indicated in Figure 5, this threshold value may be higher than the Dupré energy, W, for reasons discussed in connection with eq 1, namely, rearrangements of the interface that may enhance the interfacial energy. Such rearrangements, of course, do not affect the loading curve, where we have demonstrated in Figure 2 that we do obtain the Dupré energy from the JKR analysis. The question of whether such a low-speed asymptote for G exists must be decided experimentally and does not affect the data analysis. The reason for displaying the data in the form of Figure 5 is to illustrate that the difference between G and its threshold value, G_0, should be considered a driving force for the growth of the crack, or the shrinking of the contact radius. For a large negative value of the displacement (curve c), G grows sharply as the contact becomes unstable and the two surfaces separate.

In light of these considerations, the basic data in this paper will be presented in the format shown in Figure 6. This is another representation of the same data shown in Figures 4 and 5, where the rate dependence is included explicitly in plotting the speed, V (da/dt, time derivative of the contact radius), of shrinkage of the contact radius (the dependent variable) versus G (the driving force imposed through changes in displacement). In this figure, we see that, in fact, the data do not appear to have reached a low-speed asymptote, certainly not one in the neighborhood of $W = 2\gamma$. An important point brought out in Figure 6 is that the data in this format, that is, *the values of G associated with a particular speed of crack opening, are independent of where they are obtained on the unloading curve;* in other words, the same function, $V(G)$ is obtained for different values of δ and irrespective of whether G is instantaneously increasing or decreasing. This argues that the interface is not still undergoing time-dependent changes, resulting from rearrangements that occur on contact, when we initiate the unloading. More information on time dependence is given in the next section. This observation also argues that the properties of the interface are not nonuniform across the contact zone, for example, owing to the known variation of pressure across the zone (JKR). Silberzan et al.[23] have argued that this *is* an important feature in their data where they believe a pressure-dependent chemical reaction contributes to the adhesive energy of the interface.

(d) Contact Time Dependence. In the data displayed in Figures 4–6, there was no evident time dependence; the building of the interactions inside the contact area was finished when unloading commenced, and thus the different relaxation curves are identical in the sense that the same values of G are obtained at the same V. However, if during the unloading the interactions were to continue to build up, then the contact time would have to be taken into account. The results shown in Figure 7 come from three experiments with three different lenses. For the first lens, three steps were made 5, 8, and 12 min (curves a, b, and c, respectively) after the first contact during the initial compression. For the second lens, two steps were made after 15 and 30 min of contact (curves d and e, respectively). Clearly, the differences among these curves illustrate that there is significant evolution of the contact zone for these materials on a time scale of 30 min. Curve f, obtained after 1 h of contact, is identical to curve e and verifies that there are no significant changes after 1 h. Data such as those displayed in Figure 7 could be expanded systematically to examine the theory of O'Connor and MacLeish[24] on the kinetics of penetration of grafted chains into networks. This will be the subject of future work.

These data at early times in Figure 7 should not be used directly to determine the dependence of the G with speed of crack opening because each point corresponds to a certain contact time which in turn corresponds to a certain $G_0(t)$, representing the state of evolution of the interface that the kinetics enabled for a certain time of contact. A more complete representation of the kinetics and dynamics of interfacial adhesion development would be in a 3D display of $G(t,V)$; however, if one selects the speed from a data set such as that in Figure 7, the dependence of G, at that speed, as a function of time can be found, as shown in Figure 8. As far as we can determine, all time dependence in the data presented in this paper has run its course within 1 h of contact; therefore, all data to be presented from here on correspond to 1 h from initial contact on loading the interface. Study of longer time kinetics would require better isolation from vibrations than we employed in the present work.

Results and Discussion

The basic data of this paper should be presented in the form of measured crack opening speed, V, as a function of the driving force, which is the difference between the strain energy release rate, G, and its threshold value, G_0, as discussed in the Experimental Techniques section. Since we are unable to determine a constant value of G_0, we plot V vs G. In semilogarithmic log plots of the type we use, the shape of the

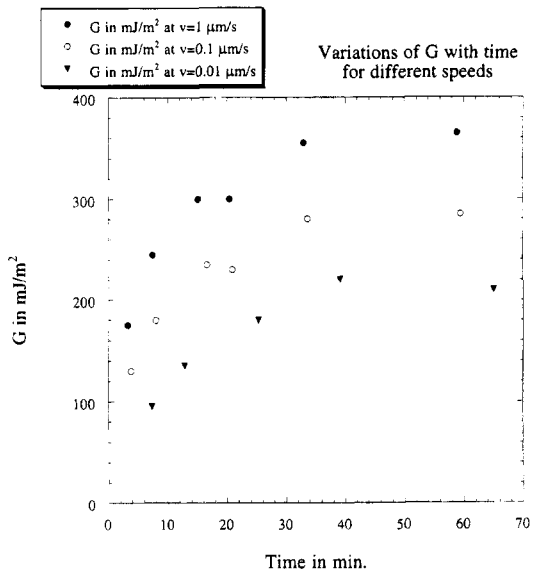

Figure 8. Data derived from Figure 7 displayed as adhesion energy as a function of contact time for different velocities of crack opening.

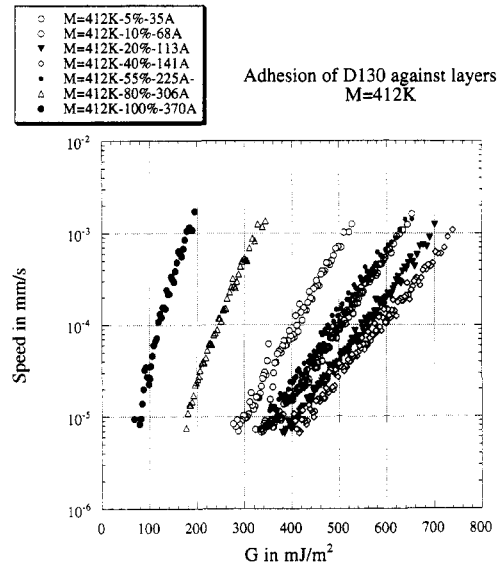

Figure 9. Data relating strain energy release rate to velocity of crack propagation for the solution-formed layers prepared at various concentrations of the grafting solution.

curves would be independent of G_0. Figure 9 shows the results obtained for solution-grafted layers of PDMS with molecular weight of 412 000. The different thicknesses obtained were grafted from different solution concentrations of the polymer, as indicated on the figure legend. Figure 10 extracts from Figure 9 the variations of G with layer thickness for three different speeds. Figure 11 displays the data for the melt-grafted layers. The different thicknesses obtained were grafted from different molecular weights, as indicated on the figure legend.

Both types of layers enhance the adhesion of the elastomeric lens to the solid surface above the PDMS surface energy. The solution-grafted layers enhance the adhesion above the level of the interaction energy of the PDMS lens with the bare wafer and, interestingly, above that achieved by the melt-grafted layers over the identical range of thickness. In order to get some idea of whether the numbers for adhesion enhancement that we get are anywhere in the neighborhood of what is anticipated by theory, we can make a simple estimate

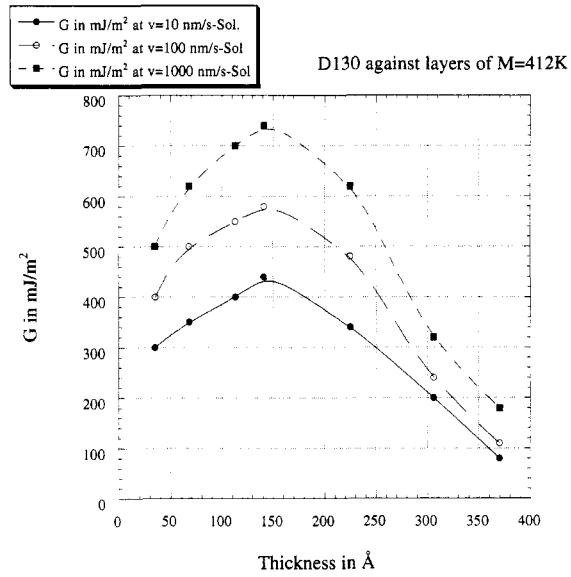

Figure 10. Data derived from Figure 9 displayed as adhesion energy as a function of the thickness of the grafted polymer layers.

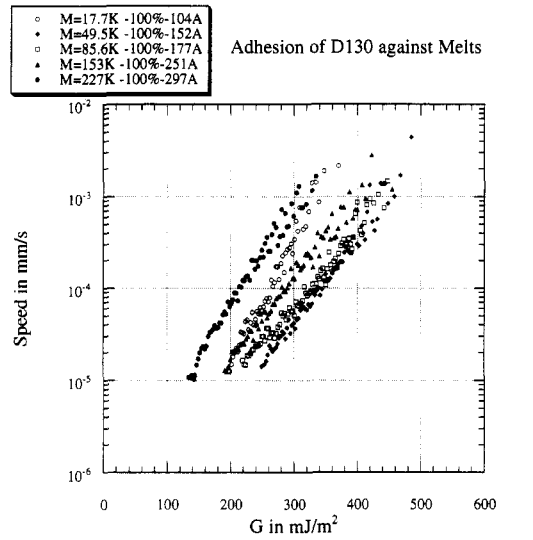

Figure 11. Data relating strain energy release rate to velocity of crack propagation for the melt-formed layers prepared at various chain lengths. These data are a portion of the total set of layers studied spanning the complete range of layer molecular weights.

of G from $G_0 \approx \gamma N \Sigma a^2$.[12] This, with $\gamma = 20$ mJ/m^2, $N = 270$, and $\Sigma a^2 = 0.06$, appropriate for the 20 000 molecular weight PDMS melt, gives $G_0 = 330$ mJ/m^2, which is in agreement with the magnitudes of values of adhesion enhancement that we measure.

Figure 12 summarizes and compares the results for the adhesion energies determined from melt- and solution-grafted layers as a function of the thickness of the grafted layers. The point at zero thickness and $G = 350$ mJ/m^2 corresponds to the adhesion of the elastomeric lens directly on a bare silicon wafer (after a contact time of 1 h, the rate dependence of this value remains to be studied in detail); the point at zero thickness and $G = 80$ mJ/m^2 corresponds to the adhesion between the elastomer and a wafer treated with a perfluorinated trichlorosilane and thereby rendered much lower in surface energy. These points are not necessarily continuations of either curve drawn in Figure 12 but are important points of reference for gauging the magnitudes of the other adhesion energies we have observed.

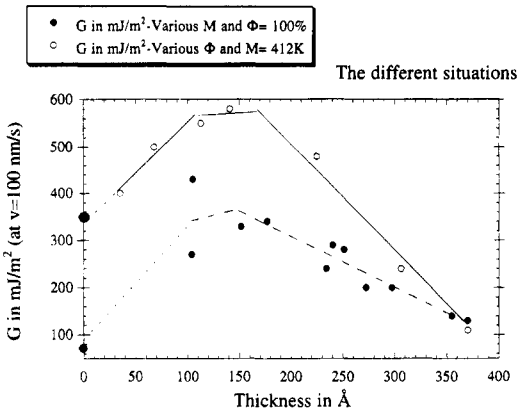

Figure 12. Data derived from Figures 9 and 11 displayed as adhesion energy as a function of the thickness of the grafted polymer layers, comparing the solution- (open symbols) and melt-formed (filled symbols) layers. The points at zero thickness (large filled circles) are not continuations of the data but are reference points, as described in the text. The lines between them and the plotted data are to guide comparison.

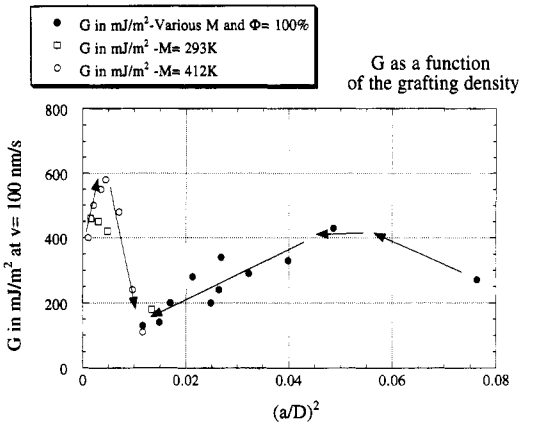

Figure 13. Data derived from Figures 9 and 11 displayed as adhesion energy as a function of the dimensionless surface density (a = 5 Å;[17] $D = \Sigma^{-2}$) of the grafted polymer layers, comparing the solution- (open symbols) and melt-formed (filled symbols) layers. The open squares are for M = 293K; the circles are for M = 412K.

The G = 80 mJ/m^2 point is higher than the value of 45 mJ/m^2 one might expect for symmetrical PDMS–PMMS contact and may reflect some imperfection in the layer. The precise value is not important; the fact that one would expect the zero-thickness point on this graph to be low is the significant issue. The data for the solution-grafted layers do not appear to extrapolate to anything like the PDMS surface energy at zero thickness. Rather, the extrapolation is to the energy corresponding to the bare wafer–elastomer interaction. It is natural that this should be the zero-thickness limit by varying the surface density. We believe that this rather high energy derives from adsorption of PDMS segments from the elastomer onto the silica via the surface hydroxyl groups. We have insufficient data to say anything about the extrapolation to zero thickness for the layers obtained from the melt. However, in the limit where numerous small molecules would be grafted to the surface, very few surface hydroxyl groups should remain and the energy should become comparable to that between the elastomer and the chlorosilane-treated surface.

We believe that the data presented here may admit more than one interpretation of may involve more than one mechanism, as we discuss below. Before going into possible interpretations in detail, we should summarize the basic experimental facts we have observed. In varying the thickness of the layer of grafted polymer, by varying the concentration of polymer in the grafting solution, Φ, *there is a pronounced maximum in the G(Σ) curves*. For the data corresponding to layers formed from the melt, a maximum is possible (especially in light of the zero-thickness reference point), but not clearly demonstrated by the present data. This maximum is not anticipated by any current model. Viewed as G as a function of thickness, the maxima for the solution-formed and melt-formed layers occur at about the same thickness (Figure 12). However, *the maxima occur at very different surface densities for the two preparation procedures* (Figure 13). The values of G we measure the solution-formed layers are generally higher than those for melt-formed layers.

Several factors may play a role in determining this unexpected behavior: chemical and physical interactions between the chains and the substrate; factors related to the swelling of the elastomer by the surface chains, and its eventual limitation at high Σ by the stretching energy of the network; kinetic barriers; chain configuration effects; and other, as-yet-unidentified phenomena. We attempt to provide some insight into these various effects in what follows.

1. The "Chemical Interactions" Point of View. The results suggest that the data at low surface coverage may contain a contribution from the wafer–lens interaction, and before we go further in the interpretation of the results, especially in terms of chain interpenetration, we have to ask ourselves about the possible contributions of chemical interactions to the observed adhesion energies. Segments of the PDMS elastomer could physisorb onto silica if they found their way to the wafer surface. The elastomer may conceivably contain some reactive groups such as hydride coming from incomplete hydrosilation or hydroxyl groups that could come from hydrolysis of hydride. The chains from the layer are OH-terminated, and there are also hydroxyl groups on the silica surface.

X-ray reflectivity studies done on this type of layer[17] show that they are dense and do not have holes. Therefore, any direct elastomer–substrate interaction implies that the elastomer penetrates or mixes with the layer. This leads us to raise (difficult-to-answer) questions about the composition of the surface region of the elastomer: Is it fully cross-linked? Does it bear any reactive groups? Are there any pendant chains and what are their molecular weights?

The first issue to address is whether the results could be explained exclusively in terms of elastomer–substrate chemical interaction. If that were the case, increasing the grafting density and thereby capping more and more hydroxyl groups on the silica surface, one would expect a decrease of the corresponding energies. This is clearly not what is always observed. We thus conclude that the interfacial chains and some mechanisms related to their physics have to be considered in order to explain the trends we observe. However, future work will have to address very carefully the relative magnitudes of effects, especially at low surface coverage.

2. The "Active Connector" Point of View. There are several reasons to expect physical phenomena associated with polymeric connector chains to play more of a role than simply joining covalent bonds. We refer to these physical actions associated with connector chains as "active connectors" or, for brevity, sometimes

just "connectors". The interdiffusion point of view supposes that the chains cross the interface and diffuse into the other medium. We note that connectors could include chains (or portions of chains) from the layer that interpenetrate the elastomer and some pendant chains (or portions) from the surface of the network that mingle with the layer. Then, when pulling the two bodies apart, one exposes the contour of the connector to air, as envisioned in the theory of de Gennes and Raphaël,[12] and one has to extend the connector and pay an energy that is proportional to the density of connectors and their length.

In the present work, we do not yet have any direct evidence of interpenetration, but interpenetration is not necessary for a connector to be active. For instance, if there were a reactive group at the end of the grafted chain or if there were even limited intermingling sufficient to produce physical entanglement, then the separation of the two bodies would lead to physical extension of the connector chains and their exposure to air with the concomitant energy cost.

In all these examples, the energy associated with the physical contribution of the active connectors would vary like the product of the length of the connectors by their surface density; in other words, it would be proprotional to the total contour length of connector chain exposed in the separation process. Therefore, in the analysis of our data, we will obtain information only on the length of the connectors that are active but not on the detailed origins of their mechanism of action.

3. The Series at Constant $\Phi = 100\%$ and Variable M. The thickness, t, of the melt-grafted layers is found experimentally by ellipsometry to vary like $t \approx aN^{1/2}$, which suggests that the chains in these layers have their unperturbed configurations (as though they were in an unconstrained melt). An increase in the thickness of the layer corresponds, in this series, to an increase in molecular weight but also to a decrease in the grafting density, Σ, which scales like $N^{-1/2}$.[16] Equation 1 gives the Raphaël–de Gennes prediction[12] that G varies with $N\Sigma$, leading to the expectation that, for these layers, G would vary with $N^{1/2}$ and, thus, G would be directly proportional to t or inversely proportional to Σ. It is impossible to say from Figure 12 whether or not a direct proportionality of G to t might exist at low thicknesses, because of insufficient data in this range. What is interesting and obvious at first sight, although at odds with the predictions, is the decrease of G with thickness above $t \approx 100$ Å.

Figure 13 replots the same data shown in Figure 12, along with additional data at another molecular weight, displaying directly the variation of G with grafting density. Confining our discussion for the moment to the melt-grafted layers (filled data points), we see that, for most of the layers, there appears to be a linear *increase* in G with Σ, in contrast to the inverse proportionality inferred from theory above. At Σ greater than about 0.06, there is a hint of the decrease anticipated above, but this is certainly not the dominant behavior we observe for this range of polymer layers.

The decrease expected by theory would ultimately lead to a value of G corresponding to the Dupré energy for pushing the lens against a close-packed monolayer of PDMS monomer, an energy which should be comparable to the energy observed for the chlorosilane-treated wafer (which is the rationale behind the dotted continuation of the melt-grafted data to zero thickness at $G =$ 80 mJ/m^2 in Figure 12).

The linearly increasing dependence of G on Σ, observed over most of the range, might suggest that, for these layers, every chain contributes to the same extent to the adhesion, independently of its molecular weight. That would mean, if the theory is applicable, that *the length of the active connector is constant and independent of the length of the grafted chain*. In other words, only a portion of a molecular chain forms an active connector.

4. The Series at Variable Φ and Constant M. The thickness of these solution-grafted layers, once they are dried, varies like $t \approx aN^{1/2}\Phi^{7/8}$,[17] since the thickness in the dried state is directly proportional to the adsorbed amount. Again referring to the predictions that G should be proportional to $N\Sigma$, we conclude that this model would predict G scaling like $N^{1/2}\Phi^{7/8}$ or, as for the melt-grafted layers, G directly proportional to t. The data at low thicknesses in Figure 12 seem to conform to this idea but, as with the melt layers, G reaches a maximum in the neighborhood of 100 Å thickness of the grafted layer.

These data are replotted, with the melt layer data, in Figure 13 as G as a function of grafting density. Notice that, although the range of thicknesses of the melt- and solution-grafted data is virtually identical, the range of grafting densities is essentially nonoverlapping. For the solution-grafted data, since molecular weight is constant, the ilnear increase in G with Σ, seen at low densities, is consistent with the theory referred to above. Again, the maximum demands a different explanation than can be found in curently available theory.

It is also important to notice that the data for the solution-grafted layers do not appear to extrapolate to anything like the PDMS surface energy at zero thickness (Figure 12) or zero grafting density (Figure 13). Rather, the extrapolation is to the energy measured for the interaction between a bare wafer and the PDMS elastomer lens. It is natural that this should be the zero-thickness limit when the limit is reached by varying surface density rather than molecular weight. However, it does also suggest that the data at low surface density may contain a contribution from the wafer–lens surface energy, in addition to the grafted layer–lens interaction. The increasing adhesion with increasing grafting shows that the chains definitely play a role in determining the adhesion energy and act as more than an inert barrier.

A point that distinguishes the melt and solution layers is the uniformly higher values of G that we find at the same thickness of layer for the solution layers. Were this only found at low thicknesses, we might conclude that the solution-grafted layers are strongly affected by direct adsorption of the network chains onto scantily covered areas of the wafer. However, we see this even at thicknesses of 200 Å. This leads us to conclude that some physical phenomenon associated with the connectors between the polymer layers is responsible for enhancing the adhesion in the solution-grafted layers.

Additional insight into the factors controlling the adhesion energy between grafted layers and cross-linked elastomeric networks is gained in examining the dependence of G on the molecular weight between cross-links in the network. For the 412 000 molecular weight melt-grafted layer, we studied adhesion to the networks made from D130, D200, and D400 whose molecular weights are given in the experimental section. We found typical values of G at $V = 0.0001$ mm/s to be 120,

165, and 340 mJ/m^2, respectively, for the three networks mentioned above. These values are very close to being in direct proportion to the molecular weights between cross-links of the three networks. Greater spacing between cross-links can produce enhanced adhesion with the identical tethered polymer layer.

5. The Adhesion Maximum. The experimental data we present here give access to the quantity, $N_c\Sigma_c$, where N_c is the number of segments in the active connector and Σ_c is the number of active connectors per unit area. Obviously, it appears from our results that N_c and Σ_c are not, in general, numerically equal to the total chain length and surface density of the tethered chains in the grafted layers on the wafer. Several possible explanations for this can be advanced.

Viewed from the standpoint of interpenetration control of adhesion, recent theoretical work by de Gennes and co-workers[25] shows that interdigitation between a brush and a network is controlled by the elasticity of the elastomer. As they endeavor to penetrate, the brush chains swell and stretch the elastomer. At some degree of interpenetration, the stretching penalty begins to be too unfavorable and interpenetration is limited. The theory developed along these lines[26] predicts that there should be a maximum. Moreover, it predicts, as we also observe, that increasing the molecular weight between cross-links in the elastomer will enhance the interpenetration and therefore the adhesion. At this point, we are unable to go beyond such a qualitative comparison because we have not measured the extent of interpenetration directly in our experiments, and furthermore, as discussed above, we have strong evidence that, even if interpenetration is involved in the adhesion enhancement mechanism, we have no independent measures of N_c and Σ_c other than that *deduced* from our data, which are, of course, not suitable for an *independent* test of the theory and which we have shown to have some differences from the actual $N\Sigma$ product.

Although not explicitly treated by the theory, the interpenetration point of view could also be related to the observation we make that solution-grafted layers enhnace adhesion more than melt-grafted layers at the same thickness. The solution-grafted layers, in the dried state in which we have employed them, are in a compressed or confirned configuration relative to chains in melt layers of the same dry thickness. This could create an enhanced driving force for intepenetration in the solution-grafted layers.[27] Any further speculation along these lines should await data on the actual degree of interpenetration that might occur in these situations.

If we return to the possibility that chemical or physical bonds are forming between the layers and the elastomers, interpenetration is not explicitly required, and one can envision several additional reasons why the product $N_c\Sigma_c$ might present a maximum. In the case of bonding interactions N_c would be the sum of contribution from the lengths of active connectors from the elastomer, $N_{c,el}$, and from the lengths of the chains of the layer, $N_{c,layer}$. For a series of experiments with different layers interacting with one network, N_c, and therefore $N_{c,layer}$, could be limited by entanglements within the layer. For the melt-grafted layers, $N_{c,layer}$ would be the entanglement length of PDMS, and, according to this view, would be constant for layers with molecular weights above the entanglement molecular weight, which was, in fact, observed (see the initial proportionality between G and Σ in Figure 13) over a range of surface chain density. For the solution-grafted layers, $N_{c,layer}$ could be higher than for melt-grafted layers of the same dry thickness, because entanglements between chains in these layers would be lower than in melt-grafted layers, thus increasing the energy of adhesion. This is a possible alternative explanation to that offered in the preceding paragraph for why the solution-grafted data lies higher than the melt-grafted data in Figure 12. On increasing the molecular weight between cross-links of the elastomer chains, $N_{c,el}$ would be expected to increase, and therefore the energy of adhesion should increase, as observed. If $N_{c,el}$ is of the same order as $N_{c,layer}$, this could lead to large changes in the energies, proportional to $N_{c,el}$, again as observed.

One should also consider possible effects of slow kinetics on the interpretation of our data. Although the data reported were obtained after 1 h of contact time, where a plateau seemed to have been reached, it is difficult to exclude the possibility of some very slow kinetics of rearrangements of the long chains in the layers, conceivably retarded also by contact with the adorbing silica surface; thus complete interdiffusion might not have occurred. Thus, finite contact time might have masked a possible dependence of $N_{c,layer}$ on the molecular weight of the pseudobrush chains.

Conclusions

The results presented in this paper lead us to conclude that the JKR method gives useful insight into the adhesion between cross-linked elastomers and polymer layers tethered on solids. The results suggest that only portions of long connector chains can be active in enhancing adhesion between elastomers and solids. These results could be interpreted in terms of interpenetration; in this case, the ability of chains from the layer to penetrate the network has to be taken into account, and the limiting factor is the elasticity of the network, as suggested by de Gennes et al.[25] Alternative interpretations to interpenetration can be given as well. Figure 13 clearly demonstrates that surface grafting density alone is not the variable controlling adhesion, at least not in the simple form envisioned by eq 1. In our opinion, this work has demonstrated several important new phenomena that ought to be exploed further in research on model systems in order to fully understand the microscopic mechanistic aspects of the observed phenomena.

Acknowledgment. We are indebted to Rhône-Poulenc Recherches and to the Center for Interfacial Engineering, an NSF-sponsored Engineering Research Center at the University of Minnesota, for financial support. The polymers used to form the elastomer lenses were kindly donated to us by Carl Kessel of 3M. We thank Martine Badeyan, Marie-Pierre Valignat, and Raymond Ober for significant assistance with the preparation and characterization of materials. This work has benefited from stimulating discussions and interactions with Miguel Aubouy, Philippe Auroy, Françoise Borchard-Wyart, Hugh Brown, Pierre-Gilles de Gennes, Edward Kramer, Yves Marciano, and Elie Raphaël.

References and Notes

(1) Pluedemann, E.; Collins, N. In *Adhesion Science and Technology*; Lee, L. H., Ed.; Plenum Press: New York, 1975.
(2) Reichert, W.; Brown, H. R. *Polymer* **1993**, *34*, 2289.
(3) Brochard-Wyart, F.; de Gennes, P.-G.; Pincus, P. *Comput. Rend. Acad. Sci. Paris* **1992**, *314*, 873.

(4) Rubinstein, M.; Adjari, A.; Leibler, L.; Brochard-Wyart, F.; de Gennes, P.-G.; Pincus, P. *Compt. Rend. Acad. Sci. Paris* **1993**, *316*, 317.
(5) Brochard-Wyart, F.; de Gennes, P.-G. *Compt. Rend. Acad. Sci. Paris* **1993**, *316*, 449.
(6) Brown, H. R. *Science* **1994**, *263*, 1411.
(7) Halperin, A.; Tirrell, M.; Lodge, T. P. *Adv. Polym. Sci.* **1992**, *100*, 31.
(8) Brown, H. R. *Annu. Rev. Mater. Sci.* **1991**, *21*, 463.
(9) Brown, H. R. *Macromolecules* **1993**, *26*, 1666.
(10) Creton, C. F.; Kramer, E. J.; Hui, C.-Y.; Brown, H. R. *Macromolecules* **1992**, *25*, 3075.
(11) Washiyama, J.; Kramer, E. J.; Creton, C. F.; Hui, C.-Y. *Macromolecules* **1994**, *27*, 2019.
(12) Raphaël, E.; de Gennes, P.-G. *J. Phys. Chem.* **1992**, *96*, 4002.
(13) Ji, H.; de Gennes, P.-G. *Macromolecules* **1993**, *26*, 520.
(14) Creton, C.; Brown, H. R.; Shull, K. *Macromolecules* **1994**, *27*, 3174.
(15) Xu, D. B.; Hui, C.-Y.; Kramer, E. J.; Creton, C. F. *Mech. Mater.* **1991**, *11*, 257.
(16) Auroy, P.; Auvray, L. *J. Phys. II* **1992**, *2*, 1133. Guiselin, O. *Europhys. Lett.* **1992**, *17*, 225.
(17) Deruelle, M.; Marciano, Y.; Tirrell, M.; Hervet, H.; Léger, L. *Faraday Discuss. Chem. Soc.* **1994**, *98*, 55. Léger, L.; Hervet, H.; Marciano, Y.; Deruelle, M.; Massey, G. *Isr. J. Chem.* **1995**, *35*, 65.
(18) Chaudhury, M. K.; Whitesides, G. M. *Langmuir* **1991**, *7*, 1013.
(19) Johnson, K. L.; Kendall, K.; Roberts, A. D. *Proc. R. Soc. London A* **1971**, *324*, 301.
(20) Maugis, D. J. *Colloid Interface Sci.* **1992**, *150*, 243.
(21) Hertz, H. J. *Reine und Angewandte Mathematik* **1882**, *92*, 156. For English translation see: *Miscellaneous Papers;* Macmillan & Co., London, 1896.
(22) Maugis, D.; Barquins, M. *J. Phys. D* **1978**, *11*, 1989.
(23) Silberzan, P.; Perutz, S.; Kramer, E. J.; Chaudhury, M. *Langmuir* **1994**, *10*, 2466.
(24) O'Connor, K. P.; MacLeish, T. C. M. *Macromolecules* **1993**, *26*, 7322.
(25) Brochard-Wyart, F.; de Gennes, P.-G.; Léger, L.; Marciano, Y.; Raphäel, E. *J. Phys. Chem.* **1994**, *98*, 9405.
(26) Aubouy, M.; Marciano, Y.; Raphaël, E.; Léger, L.; Brown, H. R., Proceedings of the 53rd International Meeting on Physical Chemistry: Organic Coatings, Paris, 1995.
(27) Watanabe, H.; Tirrell, M. *Macromolecules* **1993**, *26*, 6455.

MA946389Q